JMEPEG (2012) 21:2495–2502
DOI: 10.1007/s11665-012-0207-2

1059-9495/$19.00

Grain Refinement in Al-Mg-Si Alloy TIG Welds Using Transverse Mechanical Arc Oscillation

N.S. Biradar and R. Raman

(Submitted December 2, 2011; in revised form February 29, 2012)

Reduction in grain size in weld fusion zones (FZs) presents the advantages of increased resistance to solidification cracking and improvement in mechanical properties. Transverse mechanical arc oscillation was employed to obtain grain refinement in the weldment during tungsten inert gas welding of Al-Mg-Si alloy. Electron backscattered diffraction analysis was carried out on AA6061-AA4043 filler metal tungsten inert gas welds. Grain size, texture evolution, misorientation distribution, and aspect ratio of weld metal, PMZ, and BM have been observed at fixed arc oscillation amplitude and at three different frequencies levels. Arc oscillation showed grain size reduction and texture formation. Fine-grained arc oscillated welds exhibited better yield and ultimate tensile strengths and significant improvement in percent elongation. The obtained results were attributed to reduction in equivalent circular diameter of grains and increase in number of subgrain network structure of low angle grain boundaries.

Keywords electron backscattered diffraction, grain boundary misorientation, grain refinement, transverse mechanical arc oscillation

1. Introduction

Heat treatable wrought aluminum-magnesium-silicon (Al-Mg-Si) alloy of medium strength are extensively employed in ship building, bridge decks, and other transportation applications such as train and airplane components. Fusion welding is the most preferred welding method practiced to obtain high joint strength in these industries (Ref 1). Among aluminum alloys, Al-Mg-Si alloys appear to have weldability advantage over high strength aluminum alloys. For this reason, Al-Mg-Si alloys are widely used for structural components in welded assemblies. However, Al-Mg-Si alloys are cracking sensitive when they are autogenously fusion welded (without filler metal) (Ref 1).

To circumvent this cracking problem these alloys are welded with AA4043 filler metal, which possesses high fluidity and exhibit melting range lower than the substrate. However, when such fillers are employed the weld zone exhibits poor strength and does not respond to post-weld aging, as sufficient magnesium is not present for the precipitation of Mg_2Si, which is the main strengthening phase (Ref 2). Furthermore, fusion welding of aluminum alloys produces a FZ consisting of a cast coarse microstructure with solute gradients near the dendrite boundaries (Ref 2). In addition, strengthening precipitates are dissolved during fusion welding. These microstructural changes often lead to a significant deterioration of strength in the weld (Ref 3). Post-weld aging to restore mechanical properties is not effective because of solute loss in the matrix introduced by the solute segregation. Solution treatment and aging are needed to effectively improve the weld properties, but post-weld solution treatment is assumed to be impractical for many applications of welded components (Ref 4). Thus, attempts such as the addition of grain refiners (Ref 5, 6), electromagnetic stirring of the weld pool (Ref 7), arc pulsation (Ref 8), and arc oscillation (electro-magnetic) (Ref 9-14) have been used as alternative route to refine the grain structure of the weld metal aiming to improve its strength and reduce cracking.

Among the above-mentioned techniques, arc oscillation has been the most suitable technique under situations of design consideration of the substrate material. In the recent past, arc oscillation by electro-magnetic means has been the usual choice for many researchers, to refine weld metal structure and minimize metallurgical reactions in the weld due to associated weld thermal cycles. Metallurgical advantages of arc oscillation frequently reported in the literature, include: grain refinement in the FZ, reduced width of partially melted zone (PMZ), less distortion, control of segregation, reduced hot cracking sensitivity, reduced residual stresses, and improvement in mechanical properties (Ref 13, 14). The beneficial effect of arc oscillation was attributed to reduced net linear heat input as a result of increase in effective welding speed.

Electro-magnetic arc oscillation has been successfully used to induce grain refinement and improve weld metal properties in aluminum-lithium alloys (Ref 15), aluminum-magnesium alloys (Ref 10), and aluminum-copper alloys (Ref 11, 14). Though, many previous studies have thus addressed the problem, the reported effects of arc oscillation on weld metal grain refinement have not been consistent. For example, De Nale and Lukens (Ref 16) observed that a transverse magnetic field had a little effect on the FZ grain structure in titanium alloy GTAWs. Transverse and longitudinal arc oscillations were found to have no effect on aluminum alloys (Ref 17) and steel (Ref 13) GTAWs, while grain refinement due to arc oscillation was successfully demonstrated in aluminum-magnesium alloy

N.S. Biradar and **R. Raman**, Department of Metallurgical Engineering and Materials Science, Welding and Equipment Design Laboratory, Indian Institute of Technology, Bombay, Powai, Mumbai 400076, India. Contact e-mail: biradarns@iitb.ac.in.

welds (Ref 10, 13, 15, 18). Furthermore, some investigators (Ref 11) have expressed the difficulty of using electro-magnetic arc oscillation while welding aluminum-copper alloys (AA2014) with AC GTAW, due to inconsistent and erratic arc behavior when electromagnetic field was applied to oscillate the arc.

Considering the above-mentioned reasons, in this study, an attempt is made to demonstrate the effectiveness of arc oscillation using mechanical arc oscillator, which is referred as transverse mechanical arc oscillator (TMAO) in the following text on grain refinement in AA6061-AA4043 filler welds. The main objective of this study was to evaluate the effect of TMAO parameters on the solidification structure and mechanical properties AA6061-AA4043 filler weld metal and correlate the same with microstructural improvement, as an alternative to transverse electromagnetic arc oscillation which has not been reported so far in open literature. EBSD studies were carried out to characterize the base metal (BM) and welds in as welded condition.

2. Experimental Procedure

Al-Mg-Si commercial aluminum alloy plates provided by Bhakshi Kempharma, Thane, Mumbai of 4 mm thick were welded with AA4043 filler metal to obtain full penetration welds. Filler rod of 4 mm diameter was used based on the thickness of substrate metal and was inserted in the rectangular groove by press fitting prior to welding which was milled at the center of the substrate plate (Fig. 1). Prior to welding, the substrate plates and filler wire were mechanically brushed with wire brush to remove the tenacious oxides formed on the surface and thoroughly cleaned with acetone. The chemical composition of both substrate and filler metal is provided in Table 1.

Welding was carried out on fully automatic Square wave AC (Fronius MagicWave 2200, Austrian make) TIG welding machine. Welding current and welding speed have been chosen in such a way that the heat input for 4 mm thick plate is sufficient to result in full penetration welds. The net linear heat input for unoscillated TIG welding is calculated by the ratio of the (power × efficiency) to the welding speed. Arc oscillation amplitude and frequency were the parameters varied to obtain the beneficial effect of grain refinement which is expected to reduce net linear heat input. For arc oscillated welds, net linear heat input was calculated by the ratio of (power × efficiency) to the resultant welding speed (obtained due to the transverse oscillation of the welding torch while welding) which is higher than unoscillated weld. Arc oscillation was achieved using mechanical oscillator MO-150 (Ref 19), controller, manufactured by Jetline engineering, Inc. CA, USA. The oscillation equipment consists of a cross slide assembly with a single axis mounted on the seam weld attached to the straight mount torch and corresponding control panel. The precise movement of the cross slide on this single axis produces transverse oscillatory motion as the welding in forward motion proceeds. Control unit allows the operator to vary different oscillation speeds (frequency) and set arc amplitudes with respect to weld center line. The arc can also be oscillated either across the seam (transverse) or along the seam (longitudinal) depending upon the positioning of the cross slide assembly. In this study, arc has been oscillated transverse to the welding direction.

AA6061-AA4043 TIG TMAO welds were produced keeping amplitude constant (1.4 mm) and varying oscillation frequency levels (0.28, 0.92, and 1.5 Hz) referred as lower, medium, and higher, respectively, in the following text. Arc oscillation amplitude of 1.4 mm was fixed as this amplitude produced good weld bead morphology without any burn through (Ref 20). Table 2 gives the details of the welding and arc oscillation parameters used to prepare full penetration welds. Grain size and grain boundary characteristics were studied by EBSD technique.

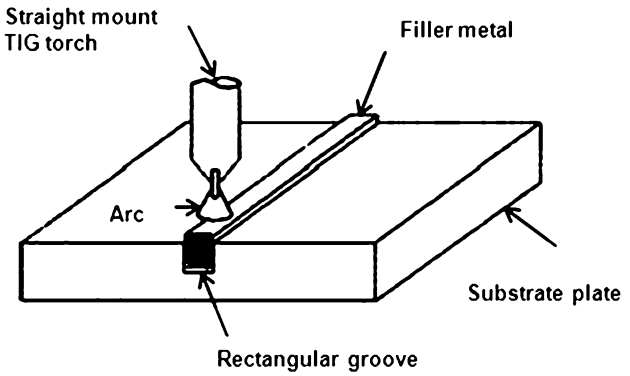

Fig. 1 Welding with filler metal preplaced in rectangular groove of the substrate metal

Table 2 Welding and TMAO parameters used to make AA6061 TIG welds of 4 mm thickness

	Welding parameters			TMAO	
Weld no	Current *I*, A	Speed *u*, mm/s	Voltage *V*, V	Amplitude, mm	Frequency, Hz
1	185	3.6	13.7	Without oscillation	
2	185	3.6	14.3	1.4	0.28
3	185	3.6	14.2	1.4	0.92
4	185	3.6	13.8	1.4	1.5

AC square wave TIG welding with constant continuous current, electrode material: W-2% Thoria, 2.4 mm diameter, AC frequency: 70 Hz, wave balance: 40/60%, arc gap: 2.4 mm, shielding gas: Ar (6-8) LPM, *Arc oscillation procedure*

Table 1 Chemical composition of the substrate and filler metal used

Material	Mn	Si	Cr	Cu	Ti	Fe	Mg	Al
AA6061 T6 (substrate)	0.10	0.18	0.22	0.04	< 0.01	0.58	1.5	Remainder
AA4043 (filler metal)	< 0.01	6	…	0.094	…	0.22	< 0.01	Remainder

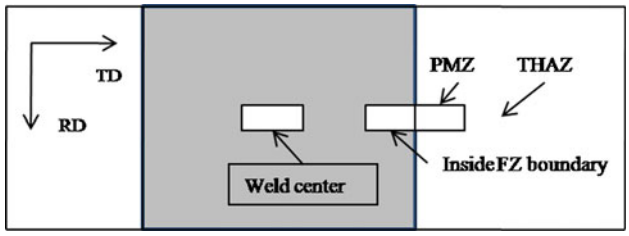

Fig. 2 Schematic diagram of weld specimen (top surface) showing locations of EBSD measurements made: weld interior, inside FZ boundary, and PMZ

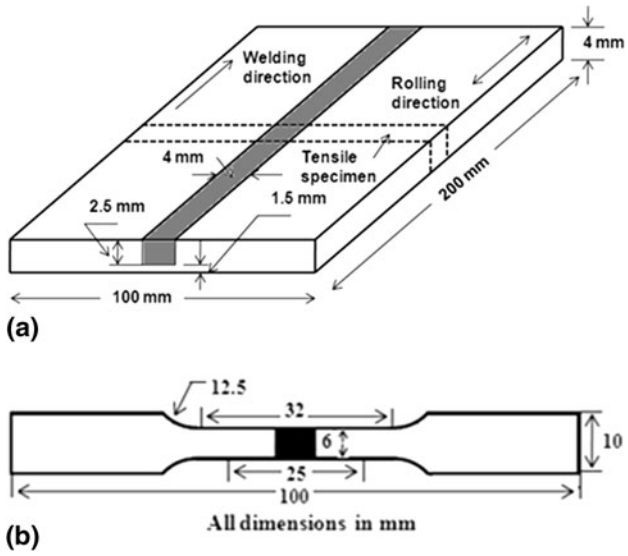

Fig. 3 Schematic of the AA6061-AA4043 filler metal weld. (a) Showing region from where tensile specimens were obtained and (b) standard subsize ASTM E8M tensile specimen (25 mm gauge length)

For EBSD characterization, each weld surface was first mechanically polished down to 0.05 μm finish with alumina and then electro-polished. Electrolytic polishing was done with 80:20; methanol:perchloric acid as electrolyte at −20 °C and 11 V DC supply. Figure 2 shows a schematic diagram of longitudinal section of the EBSD sample where scans were taken. It also shows the conventional orientations for rolling direction (RD) and travelling direction (TD). The surface analyzed was laid on the RD-TD plane.

EBSD orientation maps were obtained from different regions of the weld joint: center of FZ (weld interior), towards fusion boundary from the weld center (inside fusion boundary), and adjacent to fusion line in the heat-affected zone (HAZ), i.e., partially melted region (PMZ). EBSD measurements were obtained with Jeol 3010 microscope (300 keV operating voltage) on a FEI Quanta-200 HV SEM with TSL-EDX OIM system. Grains were identified from presence of continuous boundaries of above 5° misorientation (Ref 21). From such identified grains, grain size and grain misorientation parameters were computed. Area of the grains was calculated as: number of measurement points in a grain × (step size used in the EBSD scan)^2 × 1.5√3 (factor accounting for hexagonal grid used in the scan). The diameters of the grains were calculated by assuming a circular cross section.

Microhardness profile of the weld in the transverse direction was generated by applying a 100 g load with a Vickers indent spaced at 0.5 mm for 15 s. Measurements were carried out at approximately 2 mm below the weld surface on polished samples. Tensile specimens, from the as-welded plates, were machined according to the ASTM E8M standard, Fig. 3(b) (25 mm gauge length) and testing was carried out, at room temperature on a 100 kN MTS 810 universal testing machine at a cross head speed of 0.5 mm/min. A mean value of three test samples is reported. It is to be noted that welding was performed parallel to the RD of the plates as depicted in Fig. 3(a), thus tensile testing of the welded specimens was carried out in the RD of the plates. To make a fair comparison between the mechanical strength of the welds and that of the BM, tensile specimens of the latter were machined in the perpendicular (RD) of the plates for testing.

3. Results and Discussion

3.1 Analysis of Grain Size Using Electron Backscattered Diffraction (EBSD)

EBSD is a scanning electron microscopy (SEM)-based technique and it allows identifying the microstructure and the crystallographic orientation from a single point. Therefore, by analyzing each individual point in a designated area, one can study the grain structure, sub-structure, and grain boundary misorientations (Ref 22). Such information will not be obtained from either an optical microscope or a SEM. The purpose of the EBSD analysis was to determine whether or not any significant subgrain refinement and texture resulted during rapid solidification of the FZ material when arc oscillation was employed and correlate these changes in mechanical properties of the welds. Aluminum alloy fusion weld typically consists of FZ, HAZ consisting of PMZ and true HAZ (THAZ), and unaffected BM (Ref 23) due to the formation of unavoidable weld thermal cycles during welding. To understand the microstructural changes in these regions, EBSD measurements were made for both with and without TMAO welds.

Figure 4 shows the as-received AA6061 aluminum alloy BM microstructure. The specific crystallographic orientations of grains are typically color coded with reference to a stereographic triangle, as shown in Fig. 4(a). The IPF map obtained from the as-received BM of aluminum alloy is shown in Fig. 4(b). The image shows a deformed microstructure with average grain size, 49.45 μm with a standard deviation of 6.55 μm, and grain aspect ratio of 0.270 as estimated by the image analysis routines that are part of the EBSD software, TSL-OIM. Figure 4(b) also suggests a preferred grain orientation with strong preferential orientation for polycrystalline structure.

Figure 5 shows the EBSD orientation maps taken from top surfaces of the welds at three different locations and combined: weld interior, inside FZ boundary, and PMZ for both with and without TMAO AA6061-AA4043 filler metal welds. The color code for each of these maps is the same. Those grains that are colored blue have a ⟨100⟩ direction within 15° of being parallel to the *y*-axis, which is the vertical axis of the figures. Those grains colored red have a ⟨110⟩ direction within 15° of the *y*-axis, and those grains colored yellow have a ⟨111⟩ direction within 15° of the *y*-axis.

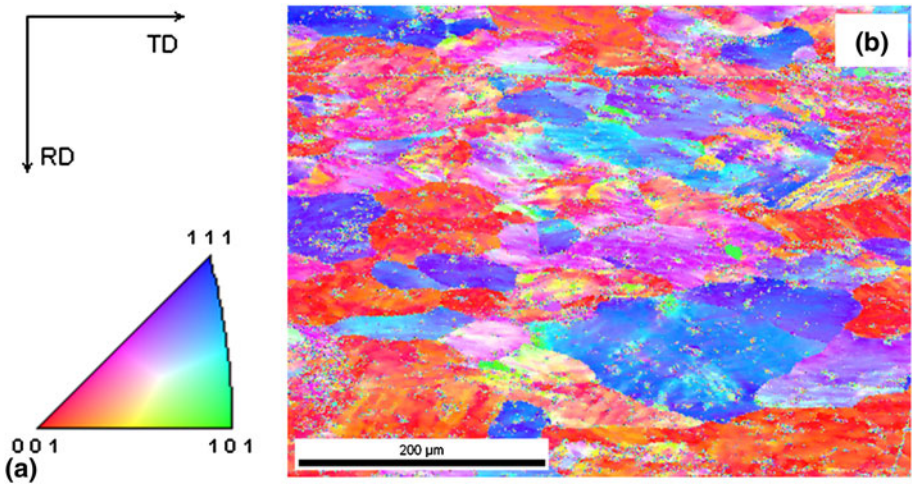

Fig. 4 EBSD map of BM. (a) stereographic triangle and (b) IPF image for as-received AA6061

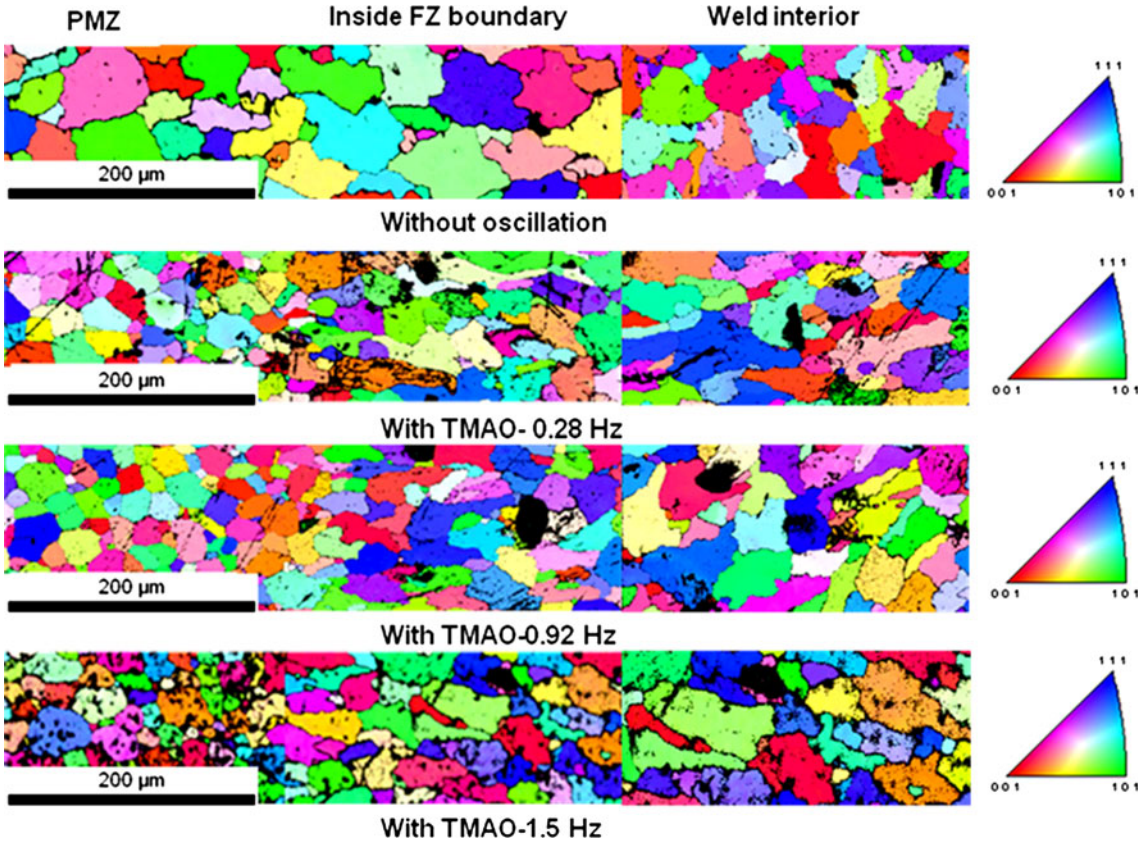

Fig. 5 EBSD orientation maps of AA6061-AA4043 filler metal welds showing regions of weld interior, inside FZ boundary, and PMZ. (a) Without oscillation and (b-d) without TMAO at constant amplitude 1.4 mm and different frequency levels (0.28-1.5 Hz)

From the EBSD orientation maps it can be concluded that TMAO results in reduction of grain size and sub grain refinement. Fine-grained microstructures obtained by TMAO of AA6061-AA4043 filler metal welds are presented in Fig. 5, along with unoscillated weld orientation map for comparison. From the equivalent circle diameter (ECD) of grains, it is seen that grain size decreased gradually from weld interior to PMZ, as depicted in Fig. 5. The color-coded orientation maps comprised both low angle grain boundary (LAGB) with average misorientation (2°-15°) and high angle grain boundary (HAGB) with (>15°) misorientation. The ECD of grains decreased from 66.36 to 54.12 µm at weld interior, 54.21 to 45.59 µm inside the FZ boundary, and 36.8 to 34.14 µm in PMZ with increase in arc oscillation frequency from 0.28 to 1.5 Hz, respectively. In comparison with grain size of 49.45 µm for BM before welding, EBSD mapping results

show the significant increases in grain size after welding which is obvious in fusion welds due to the dendritic structure of the alloy due to rapid solidification.

In the case of weld prepared without arc oscillation, due to higher heat input as compared to arc oscillated welds, Fig. 5, the measured ECD of grains in the weld interior, inside FZ boundary, and PMZ are 69.5, 63.45, and 41.3 μm, respectively. In comparison, the grain size values of TMAO welds, the results show that a decrease in (5-22%), (15-28%), and (12-20%) reduction in ECD of grains at weld interior, inside FZ boundary, and PMZ, respectively, with increase in arc oscillation frequency from lower (0.28 Hz) to higher (1.5 Hz).

The reasons for the possible change in grain structures and refinement of grains in the welds due to electro-magnetic arc oscillation have been well documented (Ref 9, 10). The above changes can be explained based on the agitation and the weld pool undergoes when the arc is made to oscillate. In case of normal welding, the solidification front is allowed to move in the direction of the steepest temperature gradient, i.e., towards the center of the arc as the welding proceeds, resulting in columnar grains and allowing the solute elements to segregate to the grain boundaries. But in case of arc oscillation the direction of steepest gradient keeps changing as the center of the arc is moved across the seam in a straight line, not allowing the grains to grow in any one direction resulting in random orientation.

3.1.1 Texture. Figure 6 shows the inverse pole figures for RD obtained from the measured orientations of weld region (inside FZ) and PMZ of AA6061-AA4043 filler metal welds prepared with and without TMAO along with AA6061 substrate alloy. As shown in Fig. 6(a), the AA6061 aluminum alloy BM before welding shows a strong preferred orientation texture. After welding, with and without TMAO at various frequency levels, the inverse pole figure shows random textures, even though the PMZ of alloy was subjected to partial melting and solidification. It can be expected that the PMZ has a solidification texture. Both regions inside FZ and PMZ of the unoscillated weld showed a strong random orientation with average misorientation angle of and 38.31° and 29.6°, respectively. However, in case of arc oscillated welds there is a gradual reduction in misorientation angle of the grains altering the randomness of the grains to preferred orientation with a minimum average misorientation of 16.43° and 11.54° in weld inside FZ and PMZ, respectively (Fig. 6e). Figure 6(a) also shows a strong alignment of mixture of [001] + [111] texture before welding. After welding, the inverse pole figure shows that the texture in weld inside FZ and PMZ becomes random (Fig. 6b) and changes to preferred orientation due application of TMAO as seen from Fig. 6(c) to (e).

3.1.2 Boundary Characteristics. Figure 7 shows the grain average misorientation distributions in AA6061 aluminum alloy and AA6061-AA4043 filler welds in all three regions of the weld joint. For AA6061 aluminum alloy, before welding the percent of HAGBs and LAGBs are 51.9 and 48.1, respectively. After welding they are 78.6 and 23.3 (weld interior), 87.4 and 12.6 (inside FZ boundary), and 68.9 and 31.1 (PMZ) regions, respectively. Due to welding (without oscillation) the percent of HAGBs increased while LAGBs reduced in all three regions (Fig. 8). On the contrary, due to TMAO welding, the percentage of HAGBs decreased while

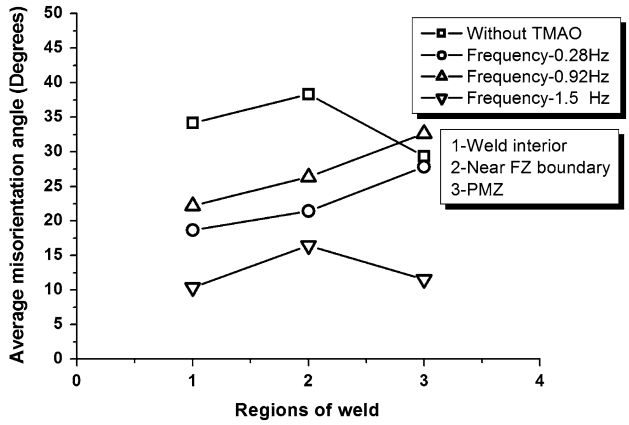

Fig. 7 Change of grain misorientation angle in AA6061-AA4043 filler metal welds prepared with and without TMAO, at three different weld regions: (1) weld interior, (2) inside FZ boundary, and (3) PMZ

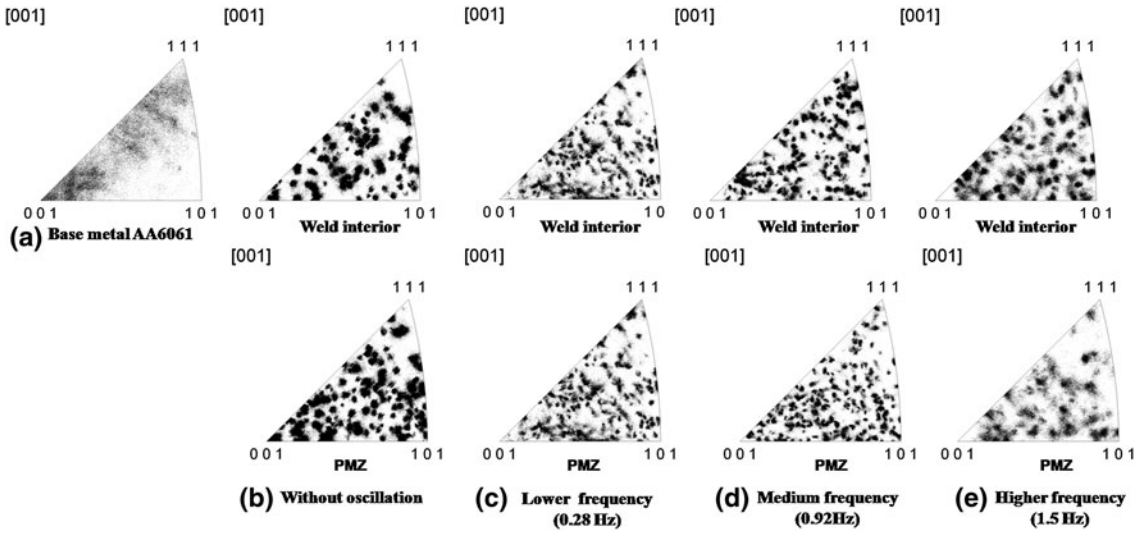

Fig. 6 RD inverse pole figures of AA6061 BM and welds prepared with and without TMAO in the PMZ

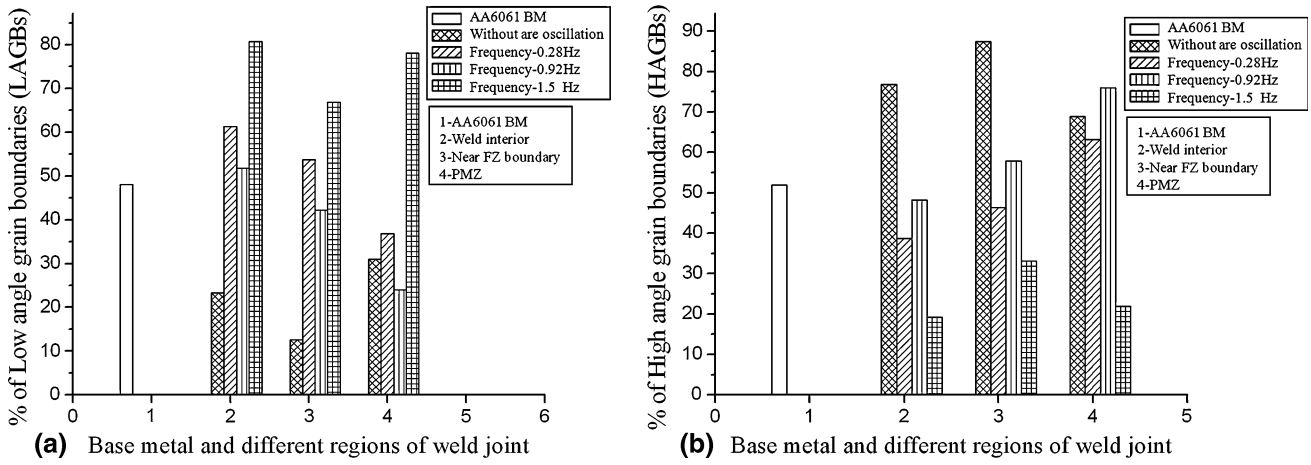

Fig. 8 Change of grain boundary characteristics in AA6061-AA4043 filler metal welds prepared with and without TMAO: (a) LAGB and (b) HAGB at three different weld regions: (1) weld interior, (2) inside FZ boundary, and (3) PMZ

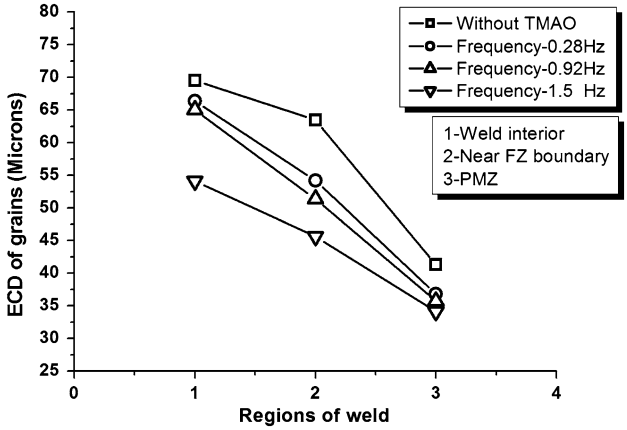

Fig. 9 Change of grain size characteristics (ECD) in AA6061-AA4043 filler metal welds prepared with and without TMAO, at three different weld regions: (1) weld interior, (2) inside FZ boundary, and (3) PMZ

increasing LAGBs in all the weld regions. It can be understood that TMAO produced higher LAGBs as compared to weld without oscillation, indicating subgrain refinement. It is to be noted that percent of subgrain boundaries increased with increase in oscillation frequency from lower to higher as seen from Fig. 8(a). The decrease of ECD (Fig. 9) of grains leads to increase in LAGBs and reduced HAGBs (Fig. 8a to b). The ratio of low angle-to-high angle boundaries increases with decreasing heat input, with increasing arc oscillation frequency. The above change in grain boundary characteristics of the solidification structure, i.e., increase in percentage of LAGBs compared to HAGBs clearly justifies that significant subgrain refinement obtained. This can be attributed physical disturbance of the weld pool structure and increase in cooling rate when TMAO was employed.

3.2 Mechanical Properties

3.2.1 Tensile Properties. Table 3 lists the BM and weld metal tensile properties. As mentioned earlier, these were determined from transverse weld tensile specimens taken from the center of the as welded plate (Fig. 3a). The refinement of the solidification structure is seen to have exercised beneficial effect on the yield and tensile strengths of the AA6061-AA4043 filler metal oscillated welds. More importantly, however, ductility has been appreciably improved by the grain refinement. This is not surprising because, while a finer grain size is known to improve ductility, its contribution to an increase in strength is marked only for very fine grain sizes (typically ≤ 5 μm) (Ref 24). It is also understood that fine equiaxed grains in weld metals of most aluminum alloys do not alter the strength of weld metals significantly, mainly because of the low value of the Hall-Petch constant (Ref 14). All the welds that were tested failed in the weld metal, and the strength of these joints was found to be proportional to the weld metal hardness values as shown in Fig. 10. As grain refinement in the weld metals could not explain the increase in the tensile and yield strengths, further investigations were made to determine the grain orientation characteristics using EBSD studies. From the EBSD orientation maps, the measured grain boundary characteristics such as LAGBs and HAGBs showed better grain orientation with increased number of LAGBs. This increase in subgrain network of LAGBs reduced the grain boundary segregation which, might have contributed to the rise in strength of the welds.

The beneficial effect of grain orientation and boundary angles, LAGB and HAGB for a polycrystalline material on mechanical properties is well documented (Ref 25). Chalmers (Ref 26) showed direct evidence for mechanical strengthening of grain boundaries on bicrystals by varying systematically the orientation difference between longitudinal grain boundaries. He observed that the yield stress of the bi-crystals increased linearly with increasing misorientation across the grain boundary, and extrapolation to zero misorientation angle gave a value close to that of the yield stress of single crystal. Parker and Washburn (Ref 27) demonstrated the effect of subgrain structure of LAGBs on stress-strain curves of 1020 steel when the material was deformed by cold working and followed by annealing. This is mainly because, LAGBs consist of simple dislocation arrays, the LAGBs move as a unit when subjected to a shear stress, in complete agreement with what is expected for a linear dislocation array. From the EBSD grain boundary measurements it is evident that arc oscillation resulted in subgrains of LAGB and the percentage of LAGBs increased

Table 3 Mechanical properties of BM AA6061 and welds made of AA6061-AA4043 filler metal

Materials	0.2% YS, MPa		UTS, MPa		% Elongation		Avg. microhardness of FZ (HV)	Failure location
	Avg.	Standard deviation	Avg.	Standard deviation	Avg.	Standard deviation		
AA6061-AA4043 filler weld without arc oscillation	99	2.08	189	3.01	13.01	0.45	69	Weld
AA6061-AA4043 filler welds with TMAO								
Lower frequency (0.28 Hz)	107	3	194	1.53	16.8	0.75	71	Weld
Medium frequency (0.92 Hz)	128	2.08	207	1.76	19.0	0.83	84	weld
Higher frequency (1.5 Hz)	100	3	199	2.29	18.24	0.68	88	Weld
AA6061 BM	210	2.02	239	2.29	24.9	1.76	81	Gage length

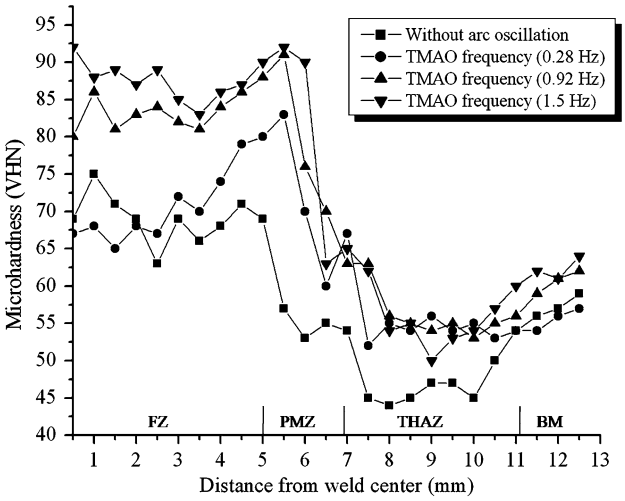

Fig. 10 Microhardness profile in transverse to the weld direction of AA6061-AA4043 filler metal welds with and without TMAO

with increase in arc oscillation frequency as shown in Fig. 8(a). This suggests that TMAO produces subgrains refinement resulting in improved tensile properties. Moreover, the ductility of the material containing a subgrain structure of LAGBs is almost as good as that of the annealed material (Ref 25).

3.2.2 Hardness. Microhardness survey was done transverse to the weld direction from weld center to BM for both welds (with and without oscillation) is shown in Fig. 10. Hardness is highest in the PMZ because this zone has fine grains compared to the FZ (Fig. 9). The hardness is lower in the THAZ portion because of particle coarsening. Softening in the THAZ of 6061 aluminum alloy is due to dissolution of strengthening β″ (Mg_2Si) precipitates (Ref 28, 29). A sharp transition in hardness occurs between immediate PMZ and THAZ. This reduction is due to dissolution of hardening β″ (Mg_2Si) particles, as these precipitates are thermodynamically unstable in a welding situation, the smallest ones will start to dissolve in the THAZ where, the peak temperature has been above ~250 °C (Ref 15).

On the other hand, TMAO welds show higher hardness values in all the regions and much smaller drop in hardness values between PMZ and THAZ when compared with the unoscillated welds. Furthermore, this relationship is further strengthened as the arc oscillation frequency increased. This could be attributed to increase in subgrain network of LAGBs (Fig. 8a) with smaller ECD of grains. Furthermore, these subgrain network with LABGs is low energy grain boundaries and they reduce the concentration of the solute distribution consequent to increase in grain boundary area.

4. Conclusions

1. TMAO can be successfully employed to obtain grain refinement in AA6061-AA4043 filler weld metals.
2. ECD of grains obtained from EBSD orientation maps clearly depicted morphological changes resulting in reduction in average grain size of the weld metal structure.
3. Frequency of TMAO seems to be playing a key role in obtaining fine grain structures. Oscillation frequency in the range (0.9-1.5 Hz) was found to be effective in reducing ECD of grains in the weld metal, inside FZ region and in the adjacent PMZ.
4. The reduction in average grain size as measured from ECD of grains improved ductility appreciably, but had lesser effect on the strength.
5. EBSD misorientation measurements from orientation maps produced subgrain network with significant increase in LAGBs, which had beneficial effect on the strength and hardness values of the TMAO welds.
6. Reduction in average grain size (ECD) and corresponding improvement in mechanical properties were attributed to reduction in net linear heat input due to increased effective welding speed leading to higher weld cooling rate when TMAO was employed.

Acknowledgments

The authors would like to thank M/S. Bhakshi Kempharma, Thane, Mumbai for providing the alloy material AA6061 aluminum alloy for carrying out necessary experiments for the current research study.

References

1. S. Kou, *Welding Metallurgy*, 2nd ed., Wiley, New York, 2003, p 13–16
2. G. Madhusudhan Reddy, P. Mastanaiah, K. Sata Prasad, and T. Mohandas, Microstructure and Mechanical Property Correlations in AA 6061 Aluminium Alloy Friction Stir Welds, *Trans. Indian Inst. Met.*, 2009, **62**(1), p 49–58

3. V. Malin, Aluminum Welded Joints, Study of Metallurgical Phenomena in the HAZ of 6061–T6, *Weld. J.*, 1995, **74**(9), p 305-s–318-s
4. R.R. Ambriz, G. Barrera, R. García, and V.H. López, The Microstructure and Mechanical Strength of Al-6061-T6 GMA Welds Obtained with the Modified Indirect Electric Arc Joint, *Mater. Des.*, 2010, **3**, p 2978–2986
5. H. Yunjia, R.H. Frost, and D.L. Olson, Edwards, Grain Refinement of Aluminum Weld Metal, *Weld. J.*, 1989, **68**, p 280 s
6. M.J. Dvornak, R.H. Frost, and D.L. Olson, The Weldability and Grain Refinement of Al 2.2 Li 2.7 Cu Alloy, *Weld. J.*, 1989, **68**, p 327s–335s
7. J.C. Villafuerte and H.W. Kerr, Electromagnetic Stirring and Grain Refinement in Stainless Steel GTA Welds, *Weld. J.*, 1990, **69**(1), p 1s–13s
8. V. Balasubramanian, V. Ravisankar, and G. Madhusudhan Reddy, Effect of Pulsed Current and Post Weld Aging Treatment on Tensile Properties of Argon Arc Welded High Strength Aluminum Alloy, *Mater. Sci. Eng., A*, 2007, **459**, p 19–34
9. S. Kou and Y. Le, Nucleation Mechanisms and Grain Refining of Weld Metal, *Weld. J.*, 1986, **65**, p 305–313s
10. S. Kou and Y. Le, Grain Structure and Solidification Cracking in Oscillated Arc Welds of 5052 Aluminum Alloy, *Metall. Trans.*, 1985, **16A**, p 1345–1352
11. S. Kou and Y. Le, Improving Weld Quality by Low Frequency Arc Oscillation, *Weld. J.*, 1985, **64**(3), p 51s–55s
12. S. Sundaresan and G.D. Janakiram, Use of Magnetic Arc Oscillation for Grain Refinement of Gas Tungsten Arc Welds in α-β Titanium Alloys, *Sci. Technol. Weld. Joining*, 1999, **4**, p 151
13. C.-F. Tseng and W.F. Savage, The Effect of Arc Oscillation, *Weld. J.*, 1971, **51**(11), p 777–785
14. S.R. Koteswara Rao, G. Madhusudhana Reddy, M. Kamaraj, and K. Prasad Rao, Grain Refinement Through Arc Manipulation Techniques in Al-Cu Alloy GTA Welds, *Mater. Sci. Eng. A*, 2005, **404**, p 227–234
15. G. Madhusudhan Reddy, A. Gokhale, and K. Prasad Rao, Weld Microstructure Refinement in a 1441 Grade Al-Li Alloy, *J. Mater. Sci.*, 1997, **32**, p 4117–4126
16. R. DeNale, and W.E. Lukens, *Proc. of Ti-6211 Basic Research Programme, Second Conference*, B.B. Rath, B.A. MacDonald, and O.P. Arora, Ed., Office of Naval Research, Arlington, VA, 1984, p 203–228
17. S. Kou and Y. Le, Alternating Grain Orientation and Weld Solidification Cracking, *Metall. Trans. A*, 1985, **16**, p 1887–1896
18. J.G. Garland, Weld Pool Solidification and Control, *Met. Constr. Br. Weld. J.*, 1974, **6**, p 121–127
19. Operational manual "MO-150 Mechanical Oscillator", Jetline engineering Inc., CA
20. N.S. Biradar, and R. Raman, *Proceedings of the IIW International Conference on Joining, Cutting, and Surfacing Technology*, D.V. Kulkarni, M. Samant, S. Krishnan, A. De, J. Krishnan, H. Patel, and A.K Bhaduri, Ed., Chennai, July 17–22, 2011, p 371–379
21. N.T. Kumbhar, S.K. Sahoo, I. Samajdar, G.K. Dey, and K. Bhanumurthy, Microstructure and Microtextural Studies of Friction Welded Aluminium Alloy 5052, *Mater. Des.*, 2011, **32**, p 1657–1666
22. Y. Zhang, S.S. Babu, P. Zhang, E.A. Kenik, and G.S. Daehn, Microstructure Characterisation of Magnetic Pulse Welded AA6061-T6 by Electron Backscattered Diffraction, *Sci. Technol. Weld. Joining*, 2008, **13**(5), p 467
23. R.W. Messler, Jr., *"Principles of Welding": Processes, Physics, Chemistry, and Metallurgy*, Wiley, New York, 1999
24. T.H. Courtney, *Mechanical Behaviour of Materials*, McGraw-Hill, Singapore, 1990, p 17
25. G.E. Dieter, *Mechanical Metallurgy*, McGraw-Hill Book Company, Singapore, 1988, p 195–197
26. R. Clark and B. Chalmers, Mechanical of Aluminium Bicrystals, *Acta Metallurgica*, 1954, **2**(1), p 80–86
27. C.H. Li, E.H. Edwards, J. Washburn, and E.R. Parker, Stress-Induced Movement of Crystal Boundaries, *Acta Metallurgica*, 1953, **1**(2), p 223–229
28. A. Kostrivas and J.C. Lippold, A Method for Studying Weld Fusion Boundary Microstructure Evaluation in Aluminum Alloys, *Weld. J.*, 2000, **79**(1), p 1s–8s
29. A. Hirosc, H. Todaka, H. Yamaoka, N. Kurosawa, and K. Kobayashi, Quantitative Evaluation of Softened Region in Weld Heat Affected Zones of 6061-T6 Aluminum Alloy—Characterizing of the Laser Beam Welding Process, *Metall. Mater. Trans. A*, 1999, **30A**(8), p 2115–2124